

Generating entanglement between quantum dots with different resonant frequencies based on Dipole Induced Transparency

Deepak Sridharan and Edo Waks

Department of Electrical and Computer Engineering,

IREAP and Joint Quantum Institute,

University of Maryland, College Park, Maryland 20742, USA

Abstract

We describe a method for generating entanglement between two spatially separated dipoles coupled to optical micro-cavities. The protocol works even when the dipoles have different resonant frequencies. This method is particularly important for solid-state emitters such as InAs QDs which suffer from large inhomogeneous broadening. We analyze the effects of non-idealities such as cavity frequency mismatch and imperfect cavity transmission, and show that the protocol is robust to these imperfections. Finally, we show that by tuning the cavity-waveguide coupling rate we can completely negate the effect of cavity frequency mismatch.

PACS numbers:

Generation of entanglement between qubits is an important operation for a large variety of applications in quantum information processing. Such states can be used to realize schemes such as transmission of secret messages via quantum key distribution[1, 2] and teleportation of quantum information[3, 4, 5, 6]. The exchange of entanglement between two distant parties is required for implementation of quantum repeaters [7]. Quantum repeaters use a combination of entanglement swapping and entanglement purification[8] to achieve unconditional secure communication over arbitrarily long distances.

To date, a variety of methods have been proposed for creating entanglement between spatially separated nodes. One of the most common methods is to transmit entangled photons generated by parametric down-conversion[9]. Entanglement protocols for atomic systems have also been proposed[10, 11, 12]. Atom entanglement has the advantages that quantum information can be stored for long time periods, which is important for long distance quantum networking.

Semiconductor based approaches to quantum information processing are currently an area of great interest because they offer the potential for a compact and scalable quantum information architecture. Solid-state emitters, such as Indium Arsenide (InAs) quantum dots (QDs) can be coupled to ultra-compact cavity waveguide systems such as those based on photonic crystals [13, 14]. A major challenge in using solid-state emitters such as InAs QDs is that they suffer from enormous inhomogeneous broadening, typically caused by emitter size variation and strain fields in the host material. The inhomogeneous broadening makes it difficult to find two identical emitters. Previous protocols for generating atom entanglement require the emitters to be identical, and are thus impractical to implement in semiconductor systems.

In this paper, we describe a protocol for creating entanglement between two dipoles with different emission frequencies. This property is extremely important for semiconductor systems. The proposed protocol uses Dipole Induced Transparency (DIT)[15] to achieve the desired entanglement. DIT occurs when a dipole is coupled to an optical cavity. When the coupling is sufficiently strong, the dipole can switch a cavity from being highly transmitting to highly reflecting. The switching contrast is determined by the Purcell Factor, which is the ratio of the lifetime of the bare emitter to the modified lifetime of the cavity-coupled emitter[16]. Purcell enhancement has been observed in semiconductor emitters coupled to a variety of different micro-cavity architectures[17].

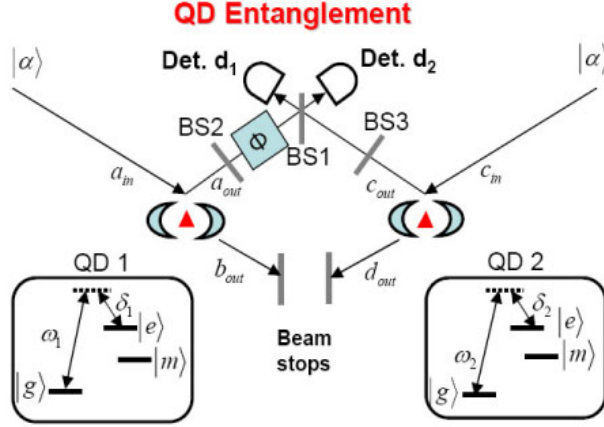


FIG. 1: Schematic of cavity waveguide system for generating entanglement between two spatially separated dipoles using DIT

The schematic for generating entanglement between two spatially separated quantum dots is shown in Figure 1. Each qubit consists of a quantum dot coupled to a double sided cavity. We define a_{in} and c_{in} as the two input modes to the cavity, and a_{out} and c_{out} as the reflected modes, and b_{out} and d_{out} as the transmitted modes. Each dipole is assumed to have three states: a ground state, a long lived metastable state and an excited state, which we refer to as $|g\rangle$, $|m\rangle$ and $|e\rangle$. The transition from the ground state to the excited state may be detuned by δ_1 and δ_2 from resonant frequencies of the two cavities, denoted by ω_1 and ω_2 respectively. The transition from the metastable state to the excited state is assumed to be decoupled from state $|e\rangle$ due to either spectral detuning or selection rules. The states $|g\rangle$ and $|m\rangle$ represent the two qubits of the system. The bare cavities have an energy decay rate of κ (in the absence of coupling to the waveguides) which is due to losses such as out-of-plane scattering and material absorption. The energy decay rates of the cavities into the reflected and transmitted modes are given by γ_1 and γ_2 respectively. The dipoles have a decay rate of $1/2\tau$.

The operators $\hat{\mathbf{a}}_{in}^\dagger$ and $\hat{\mathbf{c}}_{in}^\dagger$ are the bosonic creation operators for input flux in the top waveguide as indicated in Figure 1. They interact with the cavity-dipole system and transform the fields in the waveguide system according to the equations $\hat{\mathbf{a}}_{out}^\dagger = A_g(\omega)\hat{\mathbf{a}}_{in}^\dagger$ and $\hat{\mathbf{c}}_{out}^\dagger = C_g(\omega)\hat{\mathbf{c}}_{in}^\dagger$ where[18]

$$A_g(\omega) = \frac{(-i\Delta\omega_1 + \frac{\kappa}{2} + \frac{\gamma_2}{2} - \frac{\gamma_1}{2} + \frac{g^2}{-i(\Delta\omega_1 - \delta_1) + \frac{1}{2\tau}})}{(-i\Delta\omega_1 + \frac{\kappa}{2} + \frac{\gamma_2}{2} + \frac{\gamma_1}{2} + \frac{g^2}{-i(\Delta\omega_1 - \delta_2) + \frac{1}{2\tau}})} \quad (1)$$

$$C_g(\omega) = \frac{(-i\Delta\omega_2 + \frac{\kappa}{2} + \frac{\gamma_2}{2} - \frac{\gamma_1}{2} + \frac{g^2}{-i(\Delta\omega_2 - \delta) + \frac{1}{2\tau}})}{(-i\Delta\omega_2 + \frac{\kappa}{2} + \frac{\gamma_2}{2} + \frac{\gamma_1}{2} + \frac{g^2}{-i(\Delta\omega_2 - \delta) + \frac{1}{2\tau}})} \quad (2)$$

Equations 1 and 2 give the reflection of the waveguides when the dipoles are in the $|gg\rangle$ state. When the dipoles are in the $|mm\rangle$ state, they do not couple to cavities, and the reflection coefficients $A_m(\omega)$ and $C_m(\omega)$ are given by setting $g = 0$ in the above equations.

To understand how the protocol works, consider first the ideal case when the cavity resonant frequencies are the same and the dipoles are resonant with the cavities. Assume $\kappa = 0$ and $\gamma_1 = \gamma_2$. In this limit we have $A_g = C_g = F_p/(1 + F_p)$ and $A_m = C_m = 0$. The constant $F_p = 4g^2\tau/(\gamma_1 + \gamma_2)$ is called the Purcell factor. It is, in fact, the ratio of the cavity coupled dipole decay rate $2g^2/(\gamma_1 + \gamma_2)$ to the bare dipole decay rate $1/2\tau$. When $F_p \gg 1$ we have $A_g = C_g = 1$. Thus, when the dipole is in state $|g\rangle$, the field is completely reflected and when it is in state $|m\rangle$, the field is completely transmitted.

The protocol work as follows. Both dipoles are initialized to be in an equal superposition of the dipole states $|g\rangle$ and $|m\rangle$. Thus, the initial state is given by $1/2(|gg\rangle + |mm\rangle + |gm\rangle + |mg\rangle)$. A weak coherent field $|\alpha\rangle$ with frequency ω_c (the resonant frequency of the cavity) is inserted at inputs a_{in} and c_{in} . The reflected field from the two cavities is mixed on a 50/50 beamsplitter, as shown in Fig. 1, and the phase ϕ is adjusted so the two fields constructively interfere at detector $\hat{\mathbf{d}}_1$. For the moment, ignore the presence of the beamsplitters BS2 and BS3, the role of these beamsplitters will become clear later. Now, if the dipoles are in the state $|mm\rangle$, both fields are transmitted at the cavities and dissipated at beam stops. Therefore, the state $|mm\rangle$ cannot produce a detection event at $\hat{\mathbf{d}}_1$ or $\hat{\mathbf{d}}_2$. Similarly, for the state $|gg\rangle$ both fields are completely reflected and constructively interfere at detector $\hat{\mathbf{d}}_1$. Only the states $|gm\rangle$ and $|mg\rangle$ can cause a detection event at state $\hat{\mathbf{d}}_2$. Using the coefficients in Eq. 1 and 2 in the idealized limit, we see that a detection event at detector $\hat{\mathbf{d}}_2$ collapses the state of the qubits to $(|gm\rangle - |mg\rangle)/\sqrt{2}$.

We define the efficiency of the protocol as the probability of detecting a photon at detector $\hat{\mathbf{d}}_2$ normalized by the field intensity $|\alpha|^2$. For the ideal case, efficiency is .125 as 50% of the field is lost when the dipoles are in states $|gg\rangle$ and $|mm\rangle$ for which we never get clicks at $\hat{\mathbf{d}}_2$, 50% of the field drops into the bottom waveguide and another 50% is lost in the

beamsplitter BS1 which equally splits the fields between the ports $\hat{\mathbf{d}}_1$ and $\hat{\mathbf{d}}_2$. Now, consider what happens when the dipole frequencies are no longer equal. If the dipole transition frequencies are different, a detection event at $\hat{\mathbf{d}}_2$ does not leave the system in an entangled state. In this case we no longer have perfect DIT, and the fields reflected from the two cavities will have different amplitudes. This is illustrated in Fig 2a. where the reflectivity of a cavity for $\delta = 0$ and $\delta = 0.4$ THz are plotted. The difference in amplitude will result in imperfect destructive interference at the detector $\hat{\mathbf{d}}_2$. This means that there is some probability that state $|gg\rangle$ may cause a detection event at detector $\hat{\mathbf{d}}_2$, which leads to an imperfect entangled state. The state $|mm\rangle$, however, does not pose a problem as the field is transmitted to the bottom waveguide completely.

In order to regain perfect destructive interference at detector $\hat{\mathbf{d}}_2$, we need to make the field amplitudes on both sides of the beamsplitter equal. This is achieved by introducing a beamsplitter in the path of the waveguide as shown in Figure 1. If $|A(\omega)|^2 > |C(\omega)|^2$, we introduce a beamsplitter BS2 as shown in Figure 1 with transmission coefficient $|T_1(\omega)|^2 = |C(\omega)/A(\omega)|^2$. If $|A(\omega)|^2 < |C(\omega)|^2$, we introduce a beamsplitter BS3 in the path of signal on the right arm of the top waveguide with transmission coefficient $|T_2(\omega)|^2 = |A(\omega)/C(\omega)|^2$. A phase shift of $\phi(\omega) = \tan^{-1}(C(\omega)/A(\omega))$ is added in the path to make the phases on both sides equal. By this method of compensation, the resulting fields on both sides will be equal and would destructively interfere at $\hat{\mathbf{d}}_2$.

Using the above compensation scheme, a perfect Bell state is created for any dipole detunings δ_1 and δ_2 . We pay a price however, through a reduction in efficiency. When the detunings are large, the dipoles are not resonant with the incident field $|\alpha\rangle$, and therefore we achieve very weak DIT. This means that even when the dipole is in the state $|g\rangle$ most of the field is still transmitted through the cavity. Only a small fraction of the field is reflected and so the probability of detecting a dipole at detector $\hat{\mathbf{d}}_2$ is significantly reduced.

To understand the effect of dipole detuning on efficiency, we plot the calculated efficiency as a function of dipole detuning δ_2 in Fig. 2b. We use calculation parameters that are appropriate for InAs quantum dots coupled to photonic crystal defect cavities. For the calculations in the paper, we set $\gamma = 1$ THz and $\kappa = 0$. We set $g = 0.33$ THz for both the quantum dots, a value taken from finite difference time domain(FDTD) simulations of the cavity mode volume of a single defect photonic crystal cavity and the known oscillator strength of InAs QDs [19]. The dipole decay rate τ is set to 1 GHz, taken from experimental

measurements[20]. For the values of γ , κ and g , the Purcell factor is 218, which corresponds to a cavity reflectivity of 99.54% when the field is resonant with the dipole.

The incoming laser frequency is the common cavity resonant frequency ω_1 . Efficiency is limited by the larger of the two, δ_1 or δ_2 . In Fig. 2b, the efficiency is unchanged in the regions where $\delta_2 < \delta_1$. This is because it is limited by δ_1 , which is kept fixed. This explains the flat-top appearance of the efficiency curve. One can see that useful efficiencies are achievable even when the two dipoles are significantly detuned from each other.

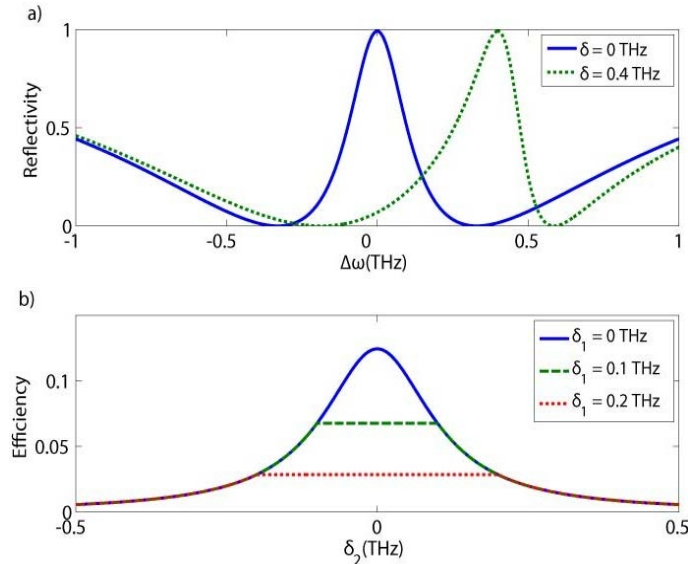


FIG. 2: a) Reflectivity of a cavity for $\delta = 0$ and $\delta = 0.4$ THz b) Efficiency as a function of δ_2 when the cavity frequencies are the same ($\omega_1 = \omega_2$)

Now let's consider the case where the two cavities down's have the same resonant frequency. In this case, it is no longer clear which frequency we should use for the coherent field $|\alpha\rangle$. In general, this can depend on both the cavity separation and dipole detunings δ_1 and δ_2 . Figure 3a plots the dependence of fidelity on the laser frequency for several different values of δ_1 . The cavity separation $\Delta\omega_s = \omega_2 - \omega_1$ is set to 0.5 THz, and $\delta_2 = \Delta\omega_s/2$ (halfway between the frequencies of the two cavities). The value of the maximum fidelity, however, is the same for all three curves, and is given by 0.84. To understand why the maximum fidelity occurs at different frequencies but is independent of δ_2 , we plot Figure 3b, the probabilities of photon detection at $\hat{\mathbf{d}}_2$ as a function of laser frequency when the dipoles are in the states $|gm\rangle$ and $|mg\rangle$ for $\delta_1 = 0.1$ THz and $\delta_2 = -0.3$ THz. The probability amplitudes for event detection at $\hat{\mathbf{d}}_2$ when the dipoles are in states $|gm\rangle$ and $|mg\rangle$ are denoted

by $G_{gm}(w)$ and $G_{mg}(w)$ respectively. Similarly, we define $G_{gg}(w)$ and $G_{mm}(w)$ to be the magnitudes of field at $\hat{\mathbf{d}}_2$ when the dipoles are in the $|gg\rangle$ and $|mm\rangle$ states. If $|G_{gg}(w)|$ and $|G_{mm}(w)|$ are small, the final state of the system is approximately given by $(G_{gm}(w)|gm\rangle - G_{mg}(w)|mg\rangle)/\sqrt{|G_{gm}(w)|^2 + |G_{mg}(w)|^2}$, given there is a detection event at $\hat{\mathbf{d}}_2$. In order to have a maximally entangled state, $G_{gm}(w)$ should be equal to $G_{mg}(w)$. This happens at a unique frequency which depends on δ_1 , δ_2 , and the cavity detuning. At the optimal frequency, $G_{gg}(w)$ is equal to 0, as it is compensated for by the beamsplitters. $G_{mm}(w)$ remains almost a constant, since it is a strong function of cavity separation which does not change for the configuration. Fidelity is given by $(G_{gm}(w) + G_{mg}(w))/\sqrt{2(|G_{gm}|^2 + |G_{mg}|^2 + |G_{mm}|^2)}$, which is maximized when $G_{gm}(w)$ is equal to $G_{mg}(w)$. Hence, we always get a maximally entangled state at the frequency where fidelity is maximum. This frequency is referred to as the optimal frequency, ω_o . In Fig 3b, $\omega_o = 0.16$ THz. For every configuration of cavity resonant frequencies and dipole detunings, there is an optimal frequency where the fidelity is maximum and G_{gm} equals G_{mg} .

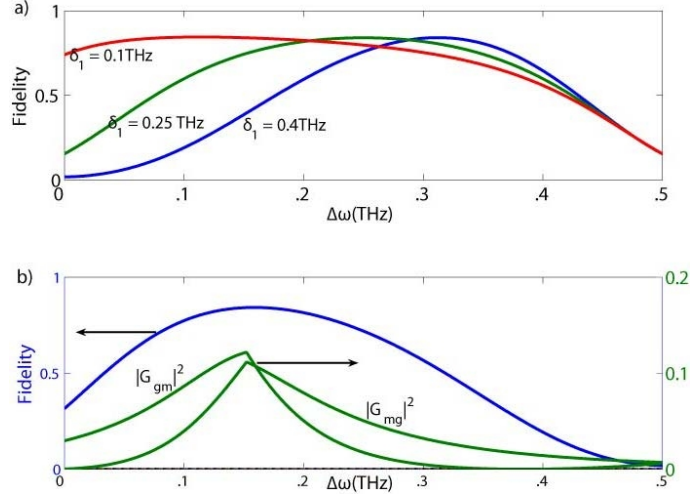


FIG. 3: a) Fidelity as a function of frequency when $\delta_2 = -0.25$ THz. The cavity separation is 0.5 THz b) Fidelity and probabilities of photon detection at $\hat{\mathbf{d}}_2$ as function of laser frequency. G_{gm} and G_{mg} are the probability amplitudes when the dipoles are in states $|gm\rangle$ and $|mg\rangle$

To understand the tradeoffs between peak fidelity and efficiency, Fig. 4a and 4b plot these two important parameters as a function of cavity detuning $\Delta\omega_s$, and dipole detuning δ_1 . The variation in δ_1 is with respect to the center frequency between the two cavities, denoted by $\omega_c = (\omega_1 + \omega_2)/2$. As Fig 4a shows, peak fidelity does not vary with dipole detuning.

However, fidelity decreases with increase in cavity separation. A maximum fidelity of 1 is achieved when the cavity separation is zero ($\Delta\omega_s = 0$). In the limit that the cavity detunings are small relative to the cavity linewidth, we can derive an approximate expression for the fidelity which is given by $1/(1+3|A(\omega)|^2)$. For a cavity separation of 0.5 THz, this expression predicts a fidelity of 0.84 which is the same as the numerically calculated value shown in the figure. From Fig 4b, maximum efficiency of .125 is obtained for the most symmetric case i.e when the dipoles are located at the ω_c .

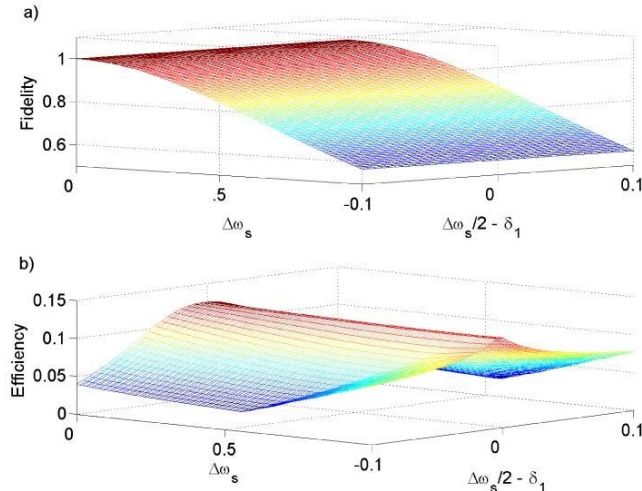


FIG. 4: (a)(b) Fidelity and efficiency as a function of cavity separations $\Delta\omega_s$ and dipole detuning δ_1

So far we have always assumed that the cavity has an equal coupling rate to both waveguides, a condition known as critical coupling. We now consider the effect of adjusting the coupling rates. We will show that by properly adjusting these rates, we can compensate for the reduction in fidelity caused by cavity detuning. This allows us to achieve high fidelity when there is a mismatch between both dipoles and cavities.

The coupling rates of the waveguides into the cavities depend on the mode overlap between the two systems. This mode overlap can be adjusted by changing the distance between the two structures, and also by tuning the hole radii near the interaction region [21].

From the equations for $A(\omega)$ and $C(\omega)$, it is evident we can lump κ and γ_2 together into one parameter, $\gamma_t = \gamma_2 + \kappa$. We typically work in the regime where $\gamma_2 \gg \kappa$, so the parameter γ_t can be tuned by changing γ_2 . Figure 5 shows the dependence of fidelity and efficiency on the coupling rate of the cavities to the bottom waveguide γ_2 for three different

δ_1 s. Maximum efficiency of .5 is achieved when $\gamma_2 = 0$ which represents the case when the bottom waveguide is absent. This is sensible because light is never transmitted, so the probability of getting a detection at detector $\hat{\mathbf{d}}_2$ is increased. However, we also have low fidelity at this point because the state $|mm\rangle$ has a high probability of creating a detection event. As γ_t is increased, the efficiency decreases but the fidelity is increased. At a certain point, the fidelity reaches a peak value of 1, indicating the creation of an ideal Bell state. All previous calculations have worked in the regime where $\gamma_2 = \gamma_1$, but as the figure shows, this is not the ideal operating point. For each value of δ_1 , there is a unique value for γ_t which achieves the optimal fidelity. This point can be better understood by considering the case when the cavities are separated by $\Delta\omega_s$ and the dipoles are located at $\Delta\omega_s/2$. For this symmetrical case, $|A_g(\omega)|$ and $|C_g(\omega)|$ are both equal, but there exists a phase difference between them. A change in γ_2 is equivalent to a change in the phase difference between the reflections from the cavities. For a particular value of γ_2 , this phase difference is equal to the phase difference between $A_m(\omega)$ and $C_m(\omega)$. At this point the phase shifter compensates for both $|gg\rangle$ and $|mm\rangle$ and we never get clicks at $\hat{\mathbf{d}}_2$. There is a γ_2 for which $G_{mm}(w) = 0$ and hence fidelity is 1.

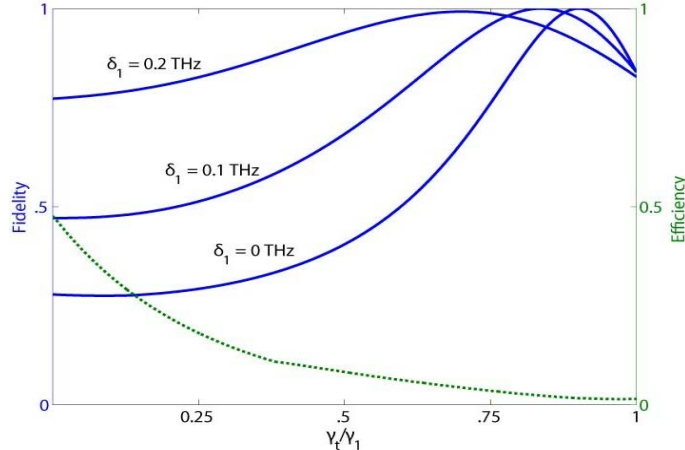


FIG. 5: Fidelity and efficiency as a function of ratio of cavity-waveguide couplings(γ_t/γ_1)(Solid lines represent fidelity and the dotted line efficiency)

In conclusion, we have shown that one can achieve high fidelity entangled states between two dipoles, even when their resonant frequencies are different. The method is robust to cavity spectral mismatch. By tuning the cavity-waveguide decay rate, we have also shown that the effect of cavity detuning can be completely nullified. The development of proto-

cols that are robust to these imperfections is extremely important for semiconductor based implementations of quantum networks.

- [1] A. K. Ekert, Phys. Rev. Lett. **67**, 661 (1991).
- [2] T. Jennewein, C. Simon, G. Weihs, H. Weinfurter, and A. Zeilinger, Phys. Rev. Lett. **84**, 4729 (2000).
- [3] C. H. Bennett et al., Phys. Rev. Lett. **70**, 1895 (1993).
- [4] D. Bouwmeester et al., Nature **390**, 595 (1997).
- [5] W. T. Buttler et al., Phys. Rev. Lett. **81**, 3283 (1998).
- [6] K. Mattle, H. Weinfurter, P. G. Kwiat, and A. Zeilinger, Phys. Rev. Lett. **76**, 4656 (1996).
- [7] H.-J. Briegel, W. Dür, J. I. Cirac, and P. Zoller, Phys. Rev. Lett. **81**, 5932 (1998).
- [8] W. Dür, H.-J. Briegel, J. I. Cirac, and P. Zoller, Phys. Rev. A **59**, 169 (1999).
- [9] P. G. Kwiat et al., Phys. Rev. Lett. **75**, 4337 (1995).
- [10] D. Jaksch, H.-J. Briegel, J. I. Cirac, C. W. Gardiner, and P. Zoller, Phys. Rev. Lett. **82**, 1975 (1999).
- [11] L.-M. Duan, M. D. Lukin, J. I. Cirac, and P. Zoller, Nature **414**, 413 (2001).
- [12] L. Childress et al., Phys. Rev. Lett. **96** (2006).
- [13] D. Englund et al., quant-ph/0609053 (2006).
- [14] D. Englund et al., Phys. Rev. Lett. **95**, 013904 (2005).
- [15] E. Waks and J. Vuckovic, Phys. Rev. Lett. **96**, 153601 (2005).
- [16] M. Pelton et al., IEEE Journal of Quantum Electronics **8**, 170 (2002).
- [17] J. M. Gérard et al., Phys. Rev. Lett. **81**, 1110 (1998).
- [18] D. Walls and G. Milburn, *Quantum Optics* (Springer, Berlin, 1994).
- [19] J. Vuckovic and Y. Yamamoto, Appl. Phys. Lett. **82**, 2374 (2003).
- [20] J. Vuckovic et al., Appl. Phys. Lett. **82** (2003).
- [21] S. Fan et al., J. Opt. Soc. Am. B **18**, 162165 (2001).